

journal homepage: <http://civiljournal.semnan.ac.ir/>

## A New Method for Drawing the Capacity Spectrum for Seismic Analysis and Structural Rehabilitation

**A. Golafshar<sup>1\*</sup>, M. H. Saghafi<sup>1</sup> and F. Eshaghi<sup>2</sup>**

1. Assistant Professor, Department of Civil Eng., Semnan Branch, Islamic Azad University, Semnan, Iran

2. Msc. Graduated of Structural Engineering, Department of Civil Eng., Semnan Branch, Islamic Azad University, Semnan, Iran

Corresponding author: [a.golafshar@semnaniau.ac.ir](mailto:a.golafshar@semnaniau.ac.ir)

### ARTICLE INFO

#### Article history:

Received: 11 November 2019

Accepted: 07 April 2020

#### Keywords:

Control point,  
Capacity spectrum,  
Effective mass.

### ABSTRACT

A review of previous studies shows that there are two general views on how to determine demand in structures through incremental nonlinear static analysis. In the first view, multi-modal methods are used to determine demand in structures. In this view, the applied load pattern is applied to the structure according to the shape of each vibration mode, assuming that the structure deformation follows the shape of the vibration mode, the capacity spectrum is drawn and after determining the target displacement and the corresponding demand for each vibration mode, the final demand is determined by combination of response modes. In the second view, structural analysis is performed as a single run nonlinear static analysis and the effect of different vibration modes is shown in one load pattern. In this method, the load pattern that has somehow the effect of different modes is applied to the structure and the structure is analyzed under this load pattern. In the second view, due to the non-conformity of the structure deformation and the lateral load of a particular vibration mode of the structure, the conventional capacity spectrum method cannot be used. Therefore, the purpose of this paper is to propose a method for drawing the capacity spectrum and determining the target displacement in single run nonlinear static analysis for non-adaptive load patterns. After presenting the equations, three frames including 3-storey, 9-storey and 20-storey frames have been selected and the results of the proposed method have been evaluated along with modal pushover method and time history analysis for the frames. Comparison of the results of the proposed method and the modal pushover with the results of the nonlinear time history analysis shows that the proposed method is more efficient in determining the lateral displacement of the stories and roof than the conventional modal pushover method.

## 1. Introduction

In the nonlinear static (pushover) analysis development, two crucial issues are considered by researchers. The first is lateral load pattern distribution for applying higher mode effects and the second is determination of target displacement. Many researchers attempt to develop pushover analysis considering higher mode effects and determination of target displacement [1-7]. For consideration of mode's changes in nonlinear range some researchers proposed adaptive methods [8-12]. Some of researchers try to develop of pushover analysis in 3D structures and Seismic response of asymmetrical and unsymmetrical buildings [13-19]. Determination of target displacement using capacity spectrum is one of the methods that has been proposed in seismic code. The development of the capacity spectrum method for determination of target displacement has been carried out by researchers in various aspects. Montez et al. [20] have proposed a method for determining the spectral displacement based on the energy input to the structure for load patterns with distribution proportional to the modal shapes. Kim et al. [21] presented a method for determining the structure response in a nonlinear static analysis with a mass proportional load pattern in which a normalized vector of a structure in elastic region has been used to determine the spectral displacement and the mass of the whole structure has been used for determining the spectral acceleration. Casarotti et al. [22] presented a method for drawing the capacity spectrum in a nonlinear static analysis with adaptive load patterns, using a displacement vector in each analysis increment, and Pinho et al. [23] evaluated its application in bridges. Wang et al. [24]

introduced the effects of soil-structure interaction in the capacity spectrum method and evaluated their proposed method for different frames. On the other hand, there are two major approaches in the studies of researchers for determining demand using incremental nonlinear static analysis. In the first method, which are called multimodal methods, the structural response is calculated by the analysis of each mode separately and the final response is obtained by combining the modes response. Multi-modal methods mainly have disadvantages, including the following.

- 1- The need for several nonlinear static analysis for structures.
- 2- In load patterns proportional to the shape of the higher vibration modes, it is possible that the roof displacement becomes opposite to the lateral load direction, which would not be possible to use the capacity spectrum method.
3. In this method, the combination of response rules, such as SRSS or CQC, is used to determine demand in the structure, which is only valid in the linear region and are imprecise when structure enters into the nonlinear region.
4. Interaction of modes in non-linear area is not considered.

In opposite to the multimodal methods, the second method is to use single run structural analysis. In the latter method, the effect of different modes of vibration is manifested in one load pattern and this load pattern is applied to the structure and the structure is analyzed under this load pattern. In the second method, due to the non-conformity of the deformation of the structure and the lateral load of a particular vibration mode of

the structure, the conventional capacity spectrum method cannot be used.

Evaluation of all developments in drawing capacity spectrum shows that a unique method for drawing capacity spectrum that applicable for various type of non-adaptive load patterns in single run nonlinear static analysis has not been proposed yet. The purpose of this paper is to provide a practical method for drawing capacity spectrum that is applicable for pushover analysis of structures with non-adaptive lateral load patterns and arbitrary distribution. In other words, the proposed method is independent of specific mode shape properties.

Considering the existence of a mass-proportional load pattern in multiple codes for incremental nonlinear static analysis of structures, this paper uses a mass-proportional load pattern as a single run load pattern for analysis and after analyzing the structures with this load pattern, the proposed method is used to determine the capacity spectrum and the target displacement. After determining the target displacement based on the proposed capacity spectrum and different earthquake demand spectra, roof lateral displacement, lateral displacement of the stories and story drifts are determined, and the mean displacement and the drift of the stories calculated by the proposed method, modal pushover and nonlinear time history analysis methods are compared and examined and their result distance compared with nonlinear time history analysis results are presented.

## 2. Drawing the Capacity Spectrum in the Conventional Method

By performing nonlinear static analysis with the distribution of force based on the shape

of the  $n^{\text{th}}$  mode, and after plotting the capacity curve (the base shear curve against the displacement of the mass center of the roof), this curve convert to capacity spectrum format. To determine the spectral displacement in the capacity spectrum in each step  $i$ , the control point displacement in the capacity curve is used, in accordance with equation (1).

$$Sd_n^i = \frac{\Delta_{cn}^i}{\Gamma_n \phi_{cn}} \quad (1)$$

$$\Gamma_n = \frac{\{\phi_n\}^T [M] \{I\}}{\{\phi_n\}^T [M] \{\phi_n\}}$$

Where  $Sd_n^i$  is spectral displacement related to the equivalent single degree of freedom structure,  $\Gamma_n$  is participation factor of the  $n^{\text{th}}$  vibration mode of multi-degree of freedom structure in the specified lateral direction,  $\phi_{cn}$  is the component of  $n^{\text{th}}$  mode shape vector at the location of the control point along the specified lateral direction,  $[M]$  is the mass matrix of the multi-degree of freedom structure and  $\{I\}$  is the vector whose components at the degrees of freedom along the ground motion has the value of unity, and zero for other components.  $\{\phi_n\}$  is the  $n^{\text{th}}$  mode shape vector. To determine the spectral acceleration in each step  $i$ , base shear  $V_n^i$  is used in equation (2).

$$Sa_n^i = \frac{V_n^i}{M_T \alpha_n} \quad (2)$$

$$\alpha_n = \frac{1}{M_T} \frac{\{\phi_n\}^T [M] \{I\}}{\{\phi_n\}^T [M] \{\phi_n\}}$$

In equation (2),  $Sa_n^i$  is the spectral acceleration associated with the equivalent single degree of freedom structure in step  $i$ ,  $M_T$  is the total mass of the multi-degree of freedom structure and  $\alpha_n$  is the effective

mass ratio of the  $n^{\text{th}}$  mode along the desired lateral direction to the total mass of the multi-degree of freedom structure. By examining equations (1) and (2), it can be seen that in the conventional method, because of the assumption that the structural deformation and lateral load pattern are followed a distribution proportional to the shape of the  $n^{\text{th}}$  mode shape of the structure, the vector of the  $n^{\text{th}}$  mode is used to determine the effective mass and draw the capacity spectrum. After drawing the capacity spectrum and bilinear approximation, by assuming that the area beneath the bilinear and real curves are equal, levels of both binary and realistic curves are equal, based on the shape of the bilinear curve, the demand spectrum is plotted with constant ductility and using the Seismosignal software [25]. After determining the appropriate intersection point in the capacity spectrum and demand, the target displacement ( $\Delta_{cnt}$ ) is calculated for the control point using equation 3.

$$\Delta_{cnt} = \Gamma_n \phi_{cn} Sd_{nt} \quad (3)$$

where  $Sd_{nt}$  is the spectral displacement in intersection of capacity and demand spectrum.

### 3. The New Proposed Method for Drawing Capacity Spectrum

In the proposed method, it is assumed that the structural analysis is performed as one run using a non-adaptive lateral load pattern. Since in this case, the deformation of the structure and the lateral load pattern do not follow a specific vibration mode of the structure, to determine the spectral displacement, the elastic deformation vector of the structure is used instead of a specific mode vector of the structure ( $n^{\text{th}}$  mode). After

pushover analysis of structures, firstly, one of the analysis steps in which the structure is in the elastic region (step e) is chosen. By substituting the structure elastic deformation vector  $\{u_e\}$  in  $e^{\text{th}}$  step instead of structure  $n^{\text{th}}$  mode shape  $\{\phi_n\}$  and substituting roof displacement  $(u_e)_{ROOF}$  in  $e^{\text{th}}$  step instead of  $\phi_{cn}$  and  $\Delta_i$  instead of  $\Delta_{cn}^i$  in equation 1, equation 4 and 5 are presented.

$$\Gamma_e = \frac{\{u_e\}^T [M] \{I\}}{\{u_e\}^T [M] \{u_e\}} \quad (4)$$

$$Sd_i = \frac{\Delta_i}{\Gamma_e \times (u_e)_{ROOF}} \quad (5)$$

In these equations  $\{u_e\}$  is the displacement vector in (step e) and  $(\Delta_i)$  is the displacement of control point in (step i).  $Sd_i$  is spectral displacement in each i step of the analysis. The parameters  $[M]$  and  $\{I\}$  are already introduced in equation (1). It should be noted that the use of structure elastic deformation vector in the calculation of spectral displacement has already been proposed by researchers [21]. In the calculation of spectral acceleration because, in the general case, the force distribution does not correspond to the structure deformation vector in the elastic region, it is not possible to use the structure deformation vector directly in relation 2 instead of the  $n^{\text{th}}$  mode vector to determine the spectral acceleration of the structure. For this purpose, to determine the spectral acceleration, the vibration frequency of the structure  $\omega_e$  is first calculated by equation 6 based on the Reighley's method [26].

$$\omega_e = \sqrt{\frac{\{u_e\}^T \{F_e\}}{\{u_e\}^T [M] \{u_e\}}} \quad (6)$$

In equation (6)  $\{F_e\}$  is lateral force vector corresponding to  $e^{\text{th}}$  step. Then in  $e^{\text{th}}$  step, the spectral displacement is determined by step 7, and given the relationship between the spectral acceleration and the spectral

displacement in the elastic region according to equation (8), the value of spectral acceleration in step  $e$   $S_{a_e}$  is obtained. By having the spectral acceleration and the base shear of the structure in step  $e^{\text{th}}$   $V_e$  and the relationship of these two parameters based on the dynamics of the structures, the effective mass  $M_{eff}$  is obtained by dividing the base shear by spectral acceleration in  $e^{\text{th}}$  step according to the equation (9). By assuming the effective mass of the structure to be constant during the analysis because of the load pattern with non-adaptive distribution, the spectral acceleration at each step  $i$   $S_{a_i}$  results from the incremental nonlinear static analysis of the base shear  $V_i$  at each step  $i$  divided on the effective mass in equation (10).

$$S_{d_e} = \frac{(u_e)_{ROOF}}{\Gamma_e \times (u_e)_{ROOF}} = \frac{1}{\Gamma_e} \quad (7)$$

$$S_{a_e} = \omega_e^2 \times S_{d_e} \quad (8)$$

$$M_{eff} = \frac{V_e}{S_{a_e}} \quad (9)$$

$$S_{a_i} = \frac{V_i}{M_{eff}} \quad (10)$$

The steps of the proposed method for drawing the capacity spectrum are as below:

1- Performing incremental nonlinear static analysis as one run with selective load pattern as Non-adaptive.

2- Determination of the base shear and roof displacement at each step of the analysis.

(  $V_i, \Delta_i$  ).

3- Selection of one of the analysis steps in which the structure is located in the elastic zone ( $e^{\text{th}}$  step). It is worth noting that, given

the proportionality of the deformation of the structure in the elastic zone, any of the structural steps in the elastic zone can be selected.

4-Determination of structure lateral deformation vector in step  $e^{\text{th}}$  ( $\{u_e\}$ )

5-Determination of lateral load vector applied on the structure in  $e^{\text{th}}$  step ( $\{F_e\}$ )

6-Determination of roof displacement in step  $e^{\text{th}}$  ( $(u_e)_{ROOF}$ )

7-Determination of structure mass matrix  $\{M\}$

8-Determination of  $\Gamma_e$  parameter based on equation 4.

9-Determination of spectral displacement in each step  $i$  of analysis based on equation (5).

10-Determination of structure vibration frequency related to deformation in  $e^{\text{th}}$  step by equation (6).

11- Determination of spectral displacement from the  $i^{\text{th}}$  step using equation (7).

12- Determination of spectral acceleration in step  $e^{\text{th}}$  using equation (8).

13- Determination of structure effective mass corresponding to  $e^{\text{th}}$  step from equation (9).

14- Determination of spectral acceleration in each  $i^{\text{th}}$  step of analysis based on equation (10).

15- Drawing capacity spectra in each  $i^{\text{th}}$  step of analysis based on parameters  $S_{a_i}$  and  $S_{d_i}$ .

In the proposed method, after determining the intersection point of the capacity spectrum and demand spectrum, the target displacement at the control point ( $\Delta_t$ ) is determined by equation (11). In equation

(11),  $Sd_t$  is the spectral displacement at intersection point of capacity and demand spectrum.

$$\Delta_t = \Gamma_e (u_e)_{ROOF} Sd_t \quad (11)$$

It should be noted that the form of equation 11 is similar to equation 3, except that the parameters  $\Gamma_n$ ,  $\phi_{cn}$  and  $Sd_m$  are substituted by  $\Gamma_n$ ,  $(u_e)_{Rc}$  and  $Sd_t$  respectively. Determination of the demand spectrum and the intersection point of the spectrum of capacity and demand is carried out based on its ideal bi-linearization, with the assumption that the surface beneath the bilinear and realistic curves are equal.

According to the bilinear curve properties, the demand spectrum is plotted with a constant ductility and the appropriate intersection point of the capacity and demand spectrums are obtained.

The proposed method can be used for the load patterns that incorporate the effects of different modes in a load pattern, so there will be no need for multiple analyses and the combination of responses in determining the final response.

## 4. Application of Proposed Method for Frames

### 4.1. Introduction of Study Frames and Modeling

In Two-dimensional frames of SAC project have been used to examine the proposed method. The studied frames consist of frames with 3, 9 and 20 stories, and the full details of the frames are presented in Gupta et al. [27]. The characteristics of the studied frames are given in Fig 1 and Table 1 to 3.

**Table 1.** Section properties of three-story frame.

Number of Stories	Beam		column	
	No	Section	No	Section
3	b1	W33x118	c1	W14x257
	b2	W30x116	c2	W14x311
	b3	W24x68	-	

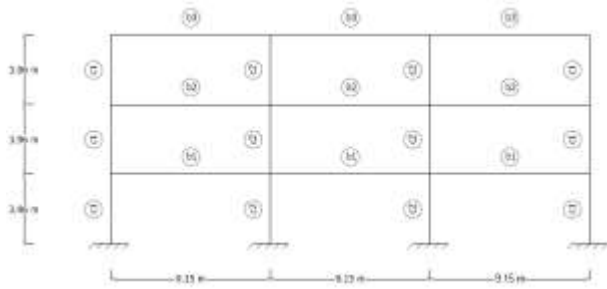
**Table 2.** Section properties of nine-story frame.

Number of Stories	Beam		column	
	No	Section	No	Section
9	b1	W36x160	c1	W14x500
	b2	W36x135	c2	W14x455
	b3	W30x99	c3	W30x370
	b4	W27x84	c4	W30x283
	b5	W24x68	c5	W30x257

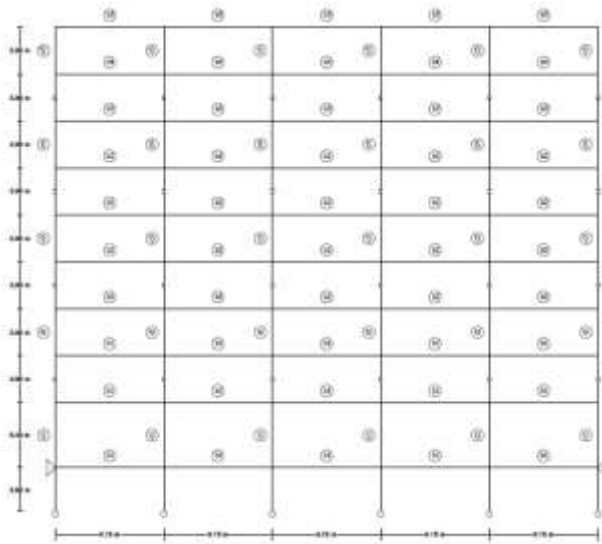
**Table 3.** Section properties of twenty-story frame.

Number of Stories	Beam		column	
	No	Section	No	Section
20	b1	W30x99	c1	w24x335
	b2	W30x108	c2	w24x229
	b3	W27x84	c3	w24x192
	b4	W24x62	c4	w24x131
	b5	W21x50	c5	w24x117
	-	-	c6	w24x84
	-	-	c7	Box 38x38x5.08
	-	-	c8	Box 38x38x3.18
	-	-	c9	Box 38x38x2.54
	-	-	c10	Box 38x38x1.91
	-	-	c11	Box 38x38x1.27

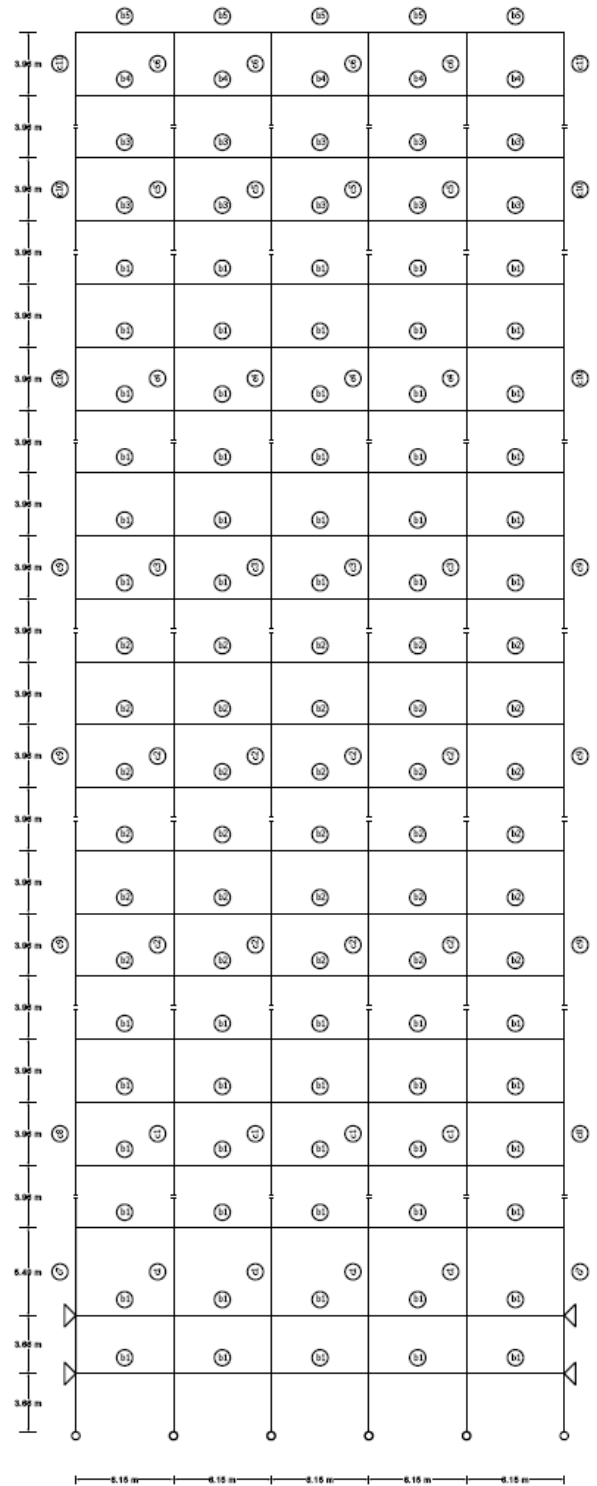
In this research, Finite element software package Sap 2000 v14[28] has been used for frames modeling. For modeling the members, frame elements are used and nonlinear behavior of the members is also considered using concentrated plasticity according to the FEMA356 [29]. The mass of the structure is also concentrated in the nodes. Comparison of the time period of vibration modes with the results of studies by Kim et al. [21] is presented in Table 4. It can be seen that the difference of results is less than 10%. Also, to further ensure the modeling process, comparison of the nonlinear behavior curves of the 3, 9 and 20-story frames in this study with the results of the studies by Kim et al. [21] are shown in Fig 2.



a)



b)

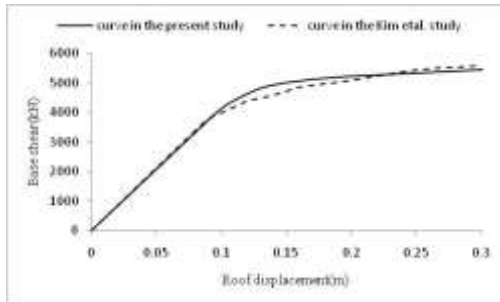


c)

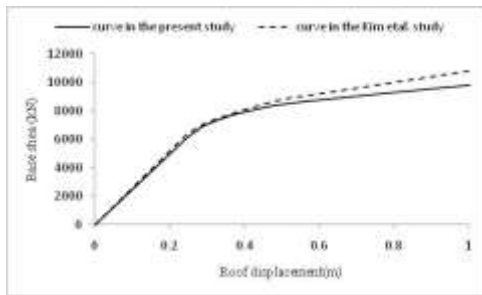
**Fig 1.** Specification of the frames a) three-story frame b) nine-story frame c) twenty-story frame.

**Table 4.** Comparison of the time period of vibration modes of the studied frames.

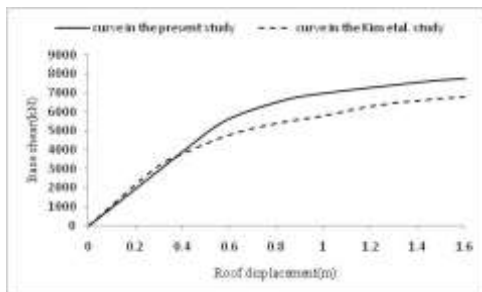
Number of Stories	The present study			Kim et al. [21]		
	First mode	Second mode	Third mode	First mode	Second mode	Third mode
3	1.07	0.35	0.19	1.01	0.33	0.17
9	2.40	0.91	0.52	2.26	0.84	0.49
20	4.09	1.44	0.84	3.96	1.37	0.79



a)



b)



c)

**Fig 2.** Comparison of pushover curve in the present study and Kim et al. study. a) three-story frame b) nine-story frame c) twenty-story frame

## 4.2. Time History Records

For nonlinear time history analysis, seven earthquake records have been used. According to the recommendations of FEMA P-695 [30], the minimum magnitude of the applied earthquakes is considered to be 6.5. The earthquake records are considered in a way that their effective time is greater than 10 seconds, in accordance with Iranian seismic code [31] recommendation. Another important parameter that influences the selection of earthquake records is the ratio between maximum acceleration and maximum velocity of earthquake record that is evaluated by Katsanose et al. [32]. Also, based on the studies conducted by Tso et al. [33] and Sawada et al [34], this parameter is related to magnitude, distance to the source and frequency content of record. Based on classification made by Tso et al. [33], the ratio between peak acceleration and peak velocity is categorized into three sub-categories.

In this study, the applied records are selected to be in the first and second categories based on the investigations of Tso et al [33].

The specifications of the selected records are shown in Table 5. In order to ensure the entry of structures to the nonlinear range, while the collapse occurrence is prevented, the selected records are scaled in such a way that the maximum displacement in the structure roof is equal to 0.015 of structure height.



**Table 5.** Specifications of the applied records.

Earthquake & station	PGA (g)	PGV (cm/s)	PGD (cm)	Soil Classification	$\frac{PGA}{PGV}$ (g/m/s)
Imperial Valley 1940/05/19 117 El Centro Array #9	0.31	29.8	13.32	C	1.05
Kocaeli, Turkey 1999/08/17 Duzce	0.36	46.4	17.61	C	0.77
Loma Prieta 1989/10/18 58224 Oakland - Title & Trust	0.24	36.1	7.2	C	0.68
Victoria, Mexico 1980/06/09 6621 Chihuahua	0.15	24.8	9.2	C	0.6
Manjil, Iran 1990-06- 20 BHRC 99999 Abhar	0.13	20.6	8.5	C	0.63
Imperial Valley 1979/10/15 5058 El Centro Array #11	0.36	34.5	16.07	C	1.06
Kocaeli, Turkey 1999/08/17 Iznik	0.14	28.8	17.44	C	0.47

### 4.3 Evaluation of the Results

Application of proposed method is carryout using mass proportional load pattern in pushover analysis of 3, 9 and 20 story frames. After performing nonlinear static analysis based on the mass-proportional load

pattern, the capacity spectrum is obtained by the proposed method and shown in Fig 3 to Fig 5. In addition to studying the proposed method in pushover nonlinear static analysis, modal pushover method proposed by Chopra et al. [1] is also used considering the influence of effective vibration modes and

the results of the proposed method and the conventional modal pushover method are compared to the results of time histories analysis for different records. For a more convenient comparison, the average results in determining the lateral displacement and the drift ratio of the stories for each method are presented.

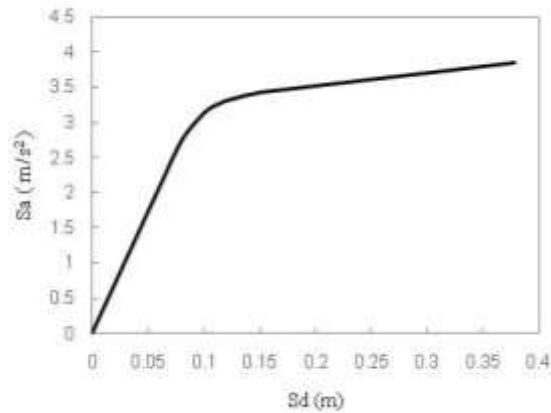


**Fig 3.** The capacity spectrum obtained by the proposed method in 3-story frame.

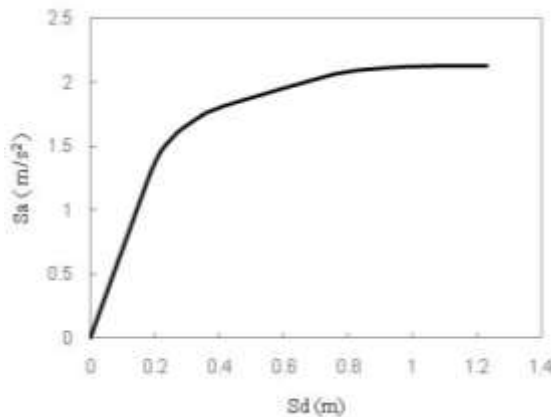


**Fig 4.** The capacity spectrum obtained by the proposed method in 9-story frame.

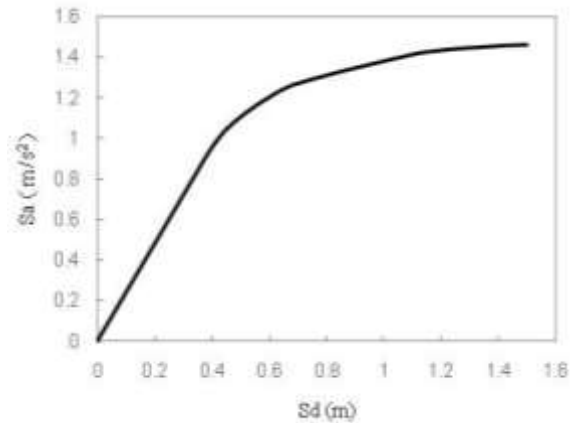


**Fig 5.** The capacity spectrum obtained by the proposed method in 20-story frame.

#### 4.3.1 Determination of Lateral Displacement of Stories in Frames

The results of the lateral displacement of the stories in the form of mean values are derived from nonlinear time histories analysis for the seven records. Comparison of story lateral displacement by the proposed method, the modal pushover and nonlinear time history analyses is shown in Fig 6 to Fig 8, and the difference between the results of static methods and the nonlinear time history analysis method are determined by equation (12) and are shown in Fig 9 to Fig 11.

$$DIFF(\%) = \frac{R_{ST} - R_{NTH}}{R_{NTH}} \times 100 \quad (12)$$

In equation (12),  $R_{ST}$  is the average response obtained from the static analysis and  $R_{NTH}$  is the average response obtained by time history analysis.

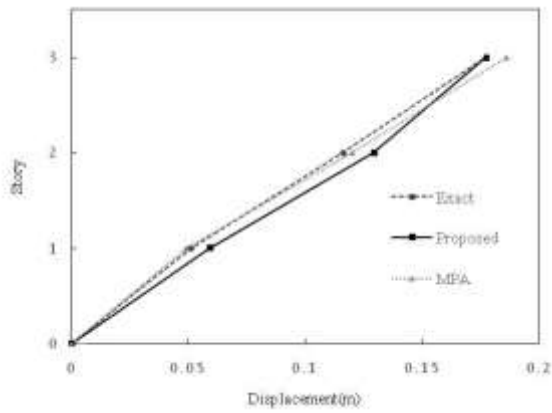


**Fig 6.** Lateral displacement of 3-story frame.

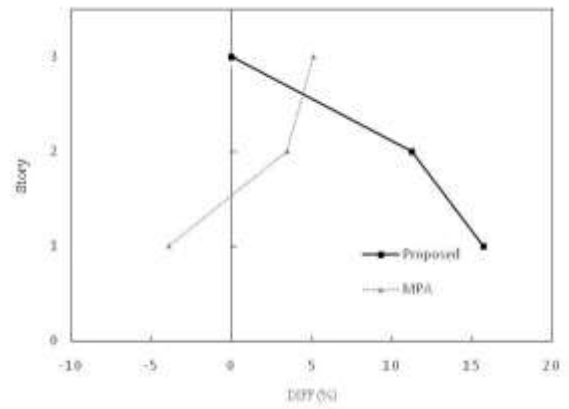


**Fig 9.** Difference between the lateral displacements of stories in 3-story frame obtained by the proposed and conventional methods.

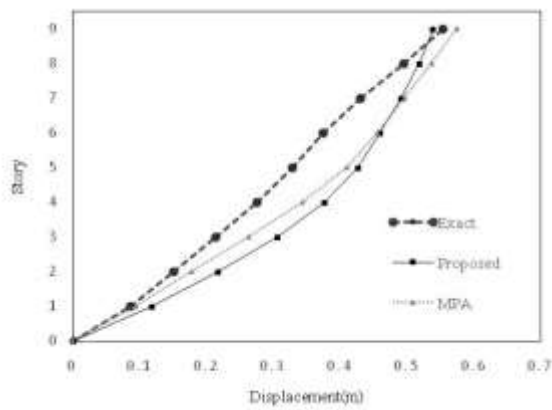


**Fig 7.** Lateral displacement of 9-story frame.

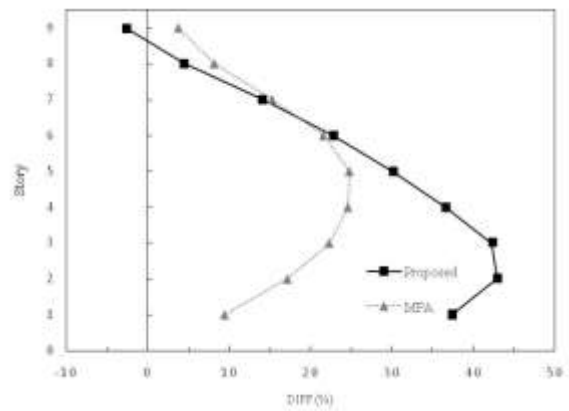


**Fig 10.** Difference between the lateral displacements of stories in 9-story frame obtained by the proposed and conventional methods.

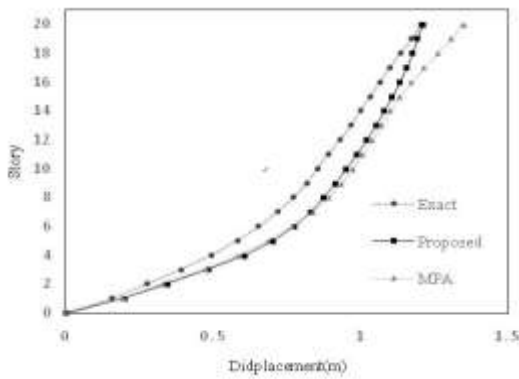


**Fig 8.** Lateral displacement of 20-story frame.

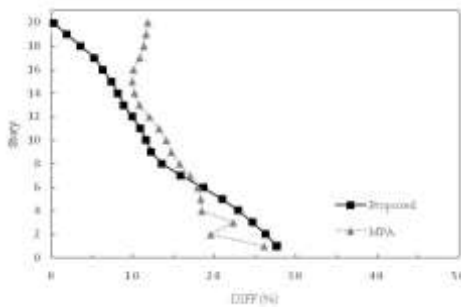


**Fig 11.** Difference between the lateral displacements of stories in 20-story frame obtained by the proposed and conventional methods.

### 4.3.2 Determination of the Drift Ratio in the Frames

Comparison of the lateral drift ratio obtained by the proposed method, the modal pushover method, and the nonlinear time history analysis is shown in Fig 12 to Fig 14 and the difference of the results of static methods compared with the results obtained by time history analysis method is calculated based on equation (12) and shown in Fig 15 to Fig 17.

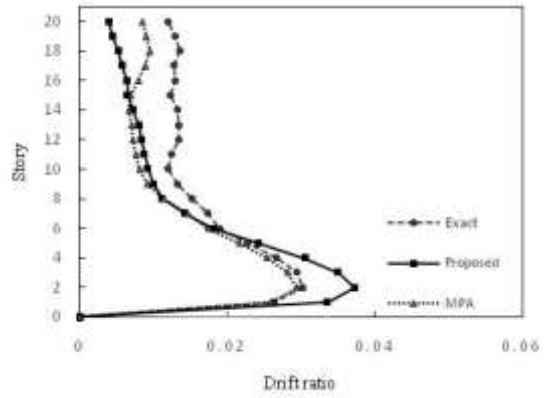


**Fig 14.** Lateral drift ratio for 20-story frame.

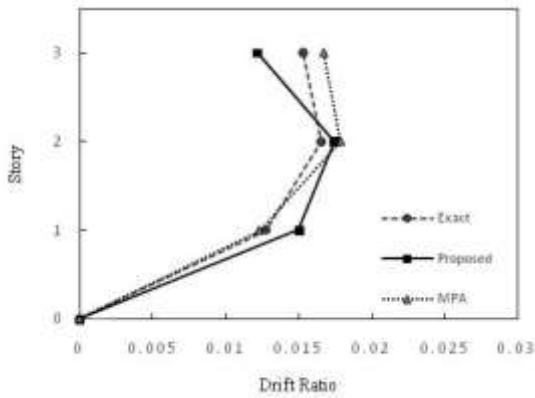


**Fig 12.** Lateral drift ratio for 3-story frame.

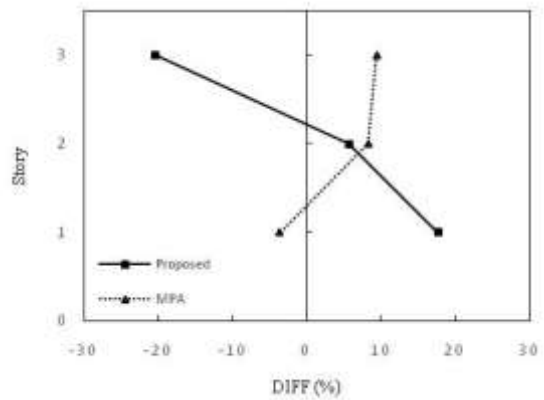


**Fig 15.** The difference in the lateral drift ratio of the stories in 3-story frame obtained by the proposed and conventional methods.

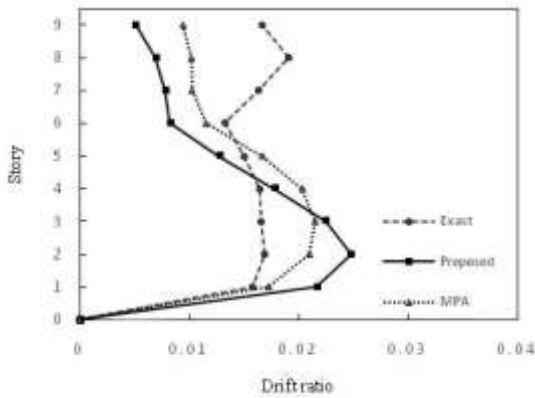


**Fig 13.** Lateral drift ratio for 9-story frame.

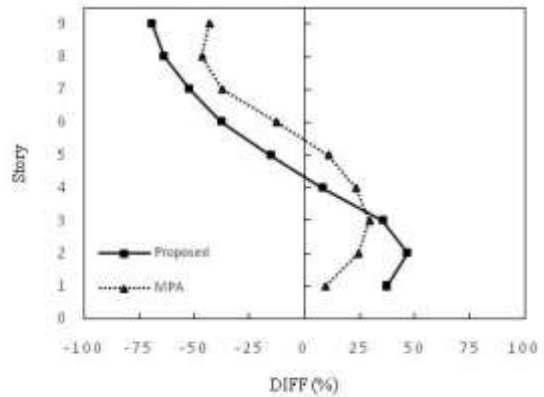


**Fig 16.** The difference in the lateral drift ratio of the stories in 9-story frame obtained by the proposed and conventional methods.

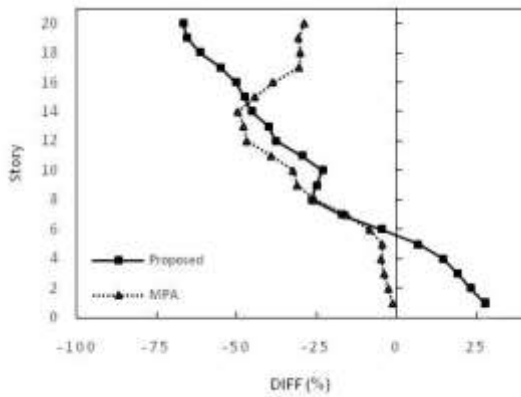


**Fig 17.** The difference in the lateral drift ratio of the stories in 20-story frame obtained by the proposed and conventional methods.

## 5. Conclusion

The purpose of this paper is to develop a capacity spectrum method to be used in load patterns with arbitrary distribution. First, the relations of the conventional method and then the proposed method relations are presented for determination of the effective mass and drawing of the capacity spectrum in the load pattern of with a distribution other than mode shapes. In the proposed method, first, the spectral displacement is determined by replacing the displacement vector of the structural in the linear region instead of the pre-specified vector of the vibration mode shape, and then the frequency of the structure in the linear region is determined based on the displacement vector, the force vector and the mass matrix. By determining the spectral displacement in the linear region along with the frequency obtained in the linear region, the spectral acceleration is estimated in the linear region and then, by dividing the base shear in the linear region by the spectral acceleration, the effective mass is determined. Having the effective mass, the spectral acceleration can be determined step

by step by dividing the base shear by effective mass. The proposed method has been evaluated in a mass proportional load pattern in three frames of 3, 9 and 20 stories and the results are compared with the results of the conventional modal pushover method and nonlinear time history analysis for seven earthquake records, and the means of the results of the methods are presented. Examining the results shows:

The proposed method, along with the mass-proportional load pattern, is more appropriate than the conventional method of modal pushover in determining the displacement of the roof point, and this is more evident in the 9- and 20-story frames.

The lateral displacement of the stories also has a mass-proportional load pattern has dispersion compared to the conventional modal pushover method for different frames and different story numbers. However, the results of the modal pushover method have lower difference in lower stories compared to the results of nonlinear time history analysis, the results of the proposed method have lower difference in upper stories compared to the results of nonlinear time history analysis.

In determination of the story drift ratio, the conventional method of the modal pushover shows a closer approximation to nonlinear time history analysis results. The reason for the difference between the results of the proposed method and the time history analysis in estimating the story drift ratio can be related to the selected lateral force distribution. The proposed method can be used for the lateral load patterns, in which the effect of various modes in a single load pattern is considered. For the determination of the structure response, there is no need for

multiple analysis and use of the mode combination.

## REFERENCES

- [1] Chopra, A. K., & Goel, R. K. (2002). "A modal pushover analysis procedure for estimating seismic demands for buildings." *Earthquake engineering & structural dynamics*, 31(3), pp. 561-582.
- [2] Shakeri, K., & Mohebbi, M. (2010). "Single-run modal pushover procedure based on the modal shear and moment in the stories." In *Proceedings of 14th European Conference on Earthquake Engineering, Ohrid, Republic of Macedonia* (pp. 6199-6207).
- [3] Poursha, M., Khoshnoudian, F., & Moghadam, A. S. (2009). "A consecutive modal pushover procedure for estimating the seismic demands of tall buildings." *Engineering Structures*, 31(2), pp. 591-599.
- [4] Vafaei, M. H., & Saffari, H. (2017). "A modal shear-based pushover procedure for estimating the seismic demands of tall building structures." *Soil Dynamics and Earthquake Engineering*, 92, pp. 95-108.
- [5] Morsali, V., Behnamfar, F. (2019). *New Lateral Force Distribution for Seismic Design of Structures Based on Seismic Demand Ratio*. *Journal of Rehabilitation in Civil Engineering*, 7(1), pp. 141-158.
- [6] FaKhraddini, A., Fadaee, M., Saffari, H. (2019). *A Target Displacement for Pushover Analysis to Estimate Seismic Demand of Eccentrically Braced Frames*. *Journal of Rehabilitation in Civil Engineering*, 7(3), pp. 103-116.
- [7] Esfahanian, A., & Aghakouchak, A. A. (2019). *A Single-Run Dynamic-Based Approach for Pushover Analysis of Structures Subjected to Near-Fault Pulse-Like Ground Motions*. *Journal of Earthquake Engineering*, 23(5), pp. 725-749.
- [8] Elnashai, A. S. (2001). "Advanced inelastic static (pushover) analysis for earthquake applications." *Structural engineering and mechanics*, 12(1), pp. 51-70.
- [9] Aydinoglu, M. N. (2003). "An incremental response spectrum analysis procedure based on inelastic spectral displacements for multi-mode seismic performance evaluation." *Bulletin of Earthquake Engineering*, 1(1), pp. 3-36.
- [10] Antoniou, S., & Pinho, R. (2004). "Development and verification of a displacement-based adaptive pushover procedure." *Journal of earthquake engineering*, 8(05), pp. 643-661.
- [11] Shakeri, K., Shayanfar, M. A., & Kabeyasawa, T. (2010). "A story shear-based adaptive pushover procedure for estimating seismic demands of buildings." *Engineering structures*, 32(1), pp. 174-183.
- [12] Abbasnia, R., Davoudi, A. T., & Maddah, M. M. (2013). "An adaptive pushover procedure based on effective modal mass combination rule." *Engineering Structures*, 52, pp. 654-666.
- [13] Reyes, J. C., & Chopra, A. K. (2011). "Three-dimensional modal pushover analysis of buildings subjected to two components of ground motion, including its evaluation for tall buildings." *Earthquake Engineering & Structural Dynamics*, 40(7), pp. 789-806.
- [14] Poursha, M., Khoshnoudian, F., & Moghadam, A. S. (2011). "A consecutive modal pushover procedure for nonlinear static analysis of one-way unsymmetric-plan tall building structures." *Engineering Structures*, 33(9), pp. 2417-2434.
- [15] Shakeri, K., Tarbali, K., & Mohebbi, M. (2012). "An adaptive modal pushover procedure for asymmetric-plan buildings." *Engineering Structures*, 36, pp. 160-172.
- [16] Rofooei, F. R., & Mirjalili, M. R. (2018). "Dynamic-based pushover analysis for one-way plan-asymmetric buildings." *Engineering Structures*, 163, 332-346.
- [17] Soleimani, S., Aziminejad, A., & Moghadam, A. S. (2017). "Extending the concept of energy-based pushover analysis to assess seismic demands of asymmetric-

- plan buildings.” *Soil Dynamics and Earthquake Engineering*, 93, pp. 29-41.
- [18] Belejo, A., & Bento, R. (2016). “Improved modal pushover analysis in seismic assessment of asymmetric plan buildings under the influence of one and two horizontal components of ground motions.” *Soil Dynamics and Earthquake Engineering*, 87, pp. 1-15.
- [19] Poursha, M., & Samarin, E. T. (2015). “The modified and extended upper-bound (UB) pushover method for the multi-mode pushover analysis of unsymmetric-plan tall buildings.” *Soil Dynamics and Earthquake Engineering*, 71, pp. 114-127.
- [20] Hernandez-Montes, E., Kwon, O. S., & Aschheim, M. A. (2004). “An energy-based formulation for first-and multiple-mode nonlinear static (pushover) analyses.” *Journal of Earthquake Engineering*, 8(01), pp. 69-88.
- [21] Kim, S. P., & Kurama, Y. C. (2008). “An alternative pushover analysis procedure to estimate seismic displacement demands.” *Engineering structures*, 30(12), pp. 3793-3807.
- [22] Casarotti, C., & Pinho, R. (2007). “An adaptive capacity spectrum method for assessment of bridges subjected to earthquake action.” *Bulletin of Earthquake Engineering*, 5(3), pp. 377-390.
- [23] Pinho, R., Monteiro, R., Casarotti, C., & Delgado, R. (2009). “Assessment of continuous span bridges through nonlinear static procedures.” *Earthquake Spectra*, 25(1), pp. 143-159.
- [24] Wang, F., & Ou, J. (2007). “Pushover analysis procedure for systems considering SSI effects based on capacity spectrum method.” *Earthquake Engineering and Engineering Vibration*, 6(3), pp. 269-279.
- [25] SeismoSoft . Seismosignal. Available from URL: <http://www.seismosoft.com>, 2011.
- [26] Lord, R. (1945). “The theory of sound.” Dover Publications, New York.
- [27] Gupta, A., & Krawinkler, H. (1998). Seismic demands for the performance evaluation of steel moment resisting frame structures (Doctoral dissertation, Stanford University).
- [28] Berkeley, C. S. I. (2011). Computer program SAP2000 v14. 2.4. Computers and Structures Inc., Berkeley, California, 80
- [29] ASCE (2000). “FEMA 356 Prestandard and Commentary for the Seismic Rehabilitation of Buildings”, ASCE for the Federal Emergency Management Agency, Washington, D.C., November 2000
- [30] FEMA P695(ATC-63),(2009), Quantification of Building Seismic Performance Factors” , Applied Technology Council , Redwoodcity ,California
- [31] Building and Housing Research Center, (2015), “Code on design of buildings against earthquakes”, Iran 2800 Standard, 4th edition.
- [32] Katsanos, E. I., Sextos, A. G., & Manolis, G. D. (2010). “Selection of earthquake ground motion records: A state-of-the-art review from a structural engineering perspective.” *Soil Dynamics and Earthquake Engineering*, 30(4), pp. 157-169.
- [33] Tso, W. K., Zhu, T. J., & Heidebrecht, A. C. (1992). “Engineering implication of ground motion A/V ratio.” *Soil Dynamics and Earthquake Engineering*, 11(3), pp. 133-144.
- [34] Sawada, T., Hirao, K., Yamamoto, H., & Tsujihara, O. (1992). “Relation between maximum amplitude ratio (a/v, ad/v 2) and spectral parameters of earthquake ground motion.” In Proc. 10th World Conf on Earthquake Engineering (Vol. 4, pp. 617-622).